Cell

SWELL1, a Plasma Membrane Protein, Is an Essential Component of Volume-Regulated Anion Channel

Zhaozhu Qiu,[1,2] Adrienne E. Dubin,[2] Jayanti Mathur,[1] Buu Tu,[1] Kritika Reddy,[1] Loren J. Miraglia,[1] Jürgen Reinhardt,[3] Anthony P. Orth,[1] and Ardem Patapoutian[2,*]
[1]Genomics Institute of the Novartis Research Foundation, San Diego, CA 92121, USA
[2]Department of Molecular and Cellular Neuroscience, Howard Hughes Medical Institute, The Scripps Research Institute, La Jolla, CA 92037, USA
[3]Novartis Institutes for Biomedical Research, Basel 4056, Switzerland
*Correspondence: ardem@scripps.edu
http://dx.doi.org/10.1016/j.cell.2014.03.024

SUMMARY

Maintenance of a constant cell volume in response to extracellular or intracellular osmotic changes is critical for cellular homeostasis. Activation of a ubiquitous volume-regulated anion channel (VRAC) plays a key role in this process; however, its molecular identity in vertebrates remains unknown. Here, we used a cell-based fluorescence assay and performed a genome-wide RNAi screen to find components of VRAC. We identified SWELL1 (LRRC8A), a member of a four-transmembrane protein family with unknown function, as essential for hypotonicity-induced iodide influx. SWELL1 is localized to the plasma membrane, and its knockdown dramatically reduces endogenous VRAC currents and regulatory cell volume decrease in various cell types. Furthermore, point mutations in SWELL1 cause a significant change in VRAC anion selectivity, demonstrating that SWELL1 is an essential VRAC component. These findings enable further molecular characterization of the VRAC channel complex and genetic studies for understanding the function of VRAC in normal physiology and disease.

INTRODUCTION

The plasma membrane of most animal cells is highly permeable to water. Increases in intracellular osmolality (e.g., during transepithelial transport, accumulation of osmolytes in metabolically active cells, and ischemic hypoxia) or decreases in extracellular osmolality will induce a rapid water influx across the cell membrane, resulting in swelling of the cell. Multiple mechanisms have been postulated to counteract the swelling and cause a regulatory volume decrease (RVD) through ion and osmolyte efflux followed by release of osmotically obligated water. For example, swelling-activated K^+ channels and K^+-Cl^- cotransporters are thought to play a role (Hoffmann et al., 2009; Lang, 2007). In addition, a large anion-selective current activated by swelling was first described in human lymphocytes three decades ago (Cahalan and Lewis, 1988; Grinstein et al., 1982) and has been subsequently observed in virtually every vertebrate cell type examined (Doroshenko and Neher, 1992; Jentsch et al., 2002; Nilius et al., 1994; Okada, 1997). Under physiological conditions, this current is primarily carried by chloride anions (and is commonly referred to as $I_{Cl,\ swell}$) but may also mediate passive efflux of small organic osmolytes, such as amino acids and their derivatives (Strange et al., 1996). The activation of $I_{Cl,\ swell}$ reduces the intracellular osmolality and constitutes one of the major pathways responsible for RVD (Hoffmann et al., 2009; Lang, 2007).

The channel underlying $I_{Cl,\ swell}$ displays a characteristic biophysical fingerprint including a low field strength anion permeability sequence ($I^- > Br^- > Cl^- > F^-$), intermediate single-channel conductance, and a mild outwardly rectifying current-voltage (*I-V*) relationship (Jentsch et al., 2002; Nilius and Droogmans, 2003; Okada et al., 2009; Strange et al., 1996). Volume-regulated anion channel (VRAC) is also referred to by other names, such as VSOR (volume-sensitive outwardly rectifying anion channel) and VSOAC (volume-sensitive organic osmolyte anion channel). Although the pharmacological and electrophysiological properties of VRAC have been described in detail, its molecular identity has remained unknown (Hoffmann et al., 2009; Nilius and Droogmans, 2003). Several candidates have been proposed to mediate $I_{Cl,\ swell}$, but none have been validated by subsequent studies (Jentsch et al., 2002; Okada et al., 1998). The lack of a specific high-affinity channel ligand hinders direct purification of the channel protein. Expression cloning, an otherwise powerful technique for ion channel identification (Hille, 2001), is severely hampered by high endogenous VRAC levels in almost all cell types, including *Xenopus* oocytes (Ackerman et al., 1994). Strong evidence supports bestrophin-1 (dBest1) as forming the *Drosophila* $I_{Cl,\ swell}$ channel (Chien and Hartzell, 2007; Stotz and Clapham, 2012). However, the biophysical properties of this channel are distinct from vertebrate VRAC (Stotz and Clapham, 2012), and $I_{Cl,\ swell}$ is unimpaired in murine cells with both mBest1 and mBest2 disrupted (Chien and Hartzell, 2008). This indicates that bestrophins are unlikely to mediate VRAC in vertebrate cells.

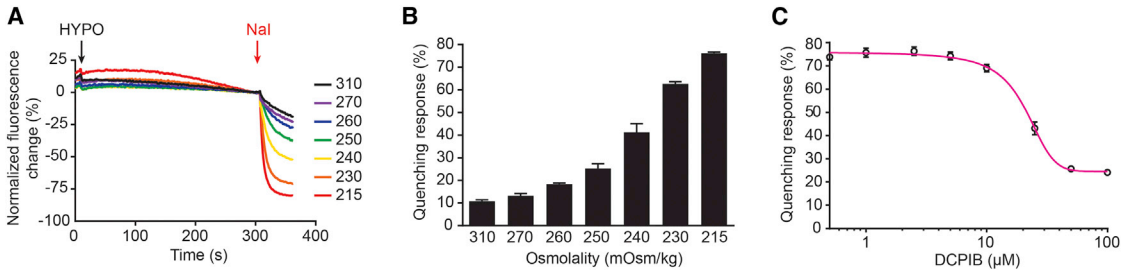

Figure 1. Hypotonicity-Induced YFP Quenching Assay

(A) Representative traces of fluorescence change (normalized to the baseline immediately before the addition of NaI) in HEK-YFP cells under different hypotonic stimuli (HYPO) in mOsm/kg as monitored by the Fluorometric Imaging Plate Reader.

(B) Hypotonicity-induced quenching responses (mean ± SEM, n = 4) during increasing hypotonic stimuli.

(C) Concentration-response relationship for DCPIB to the quenching response induced by 215 mOsm/kg. Each data point is mean ± SEM, n = 8.

See also Figure S1 and Table S1.

In this study, we established a cell-based fluorescence assay for hypotonicity-induced iodide influx and performed a genome-wide RNAi screen in HEK293T cells. This strategy has enabled us to identify SWELL1 (LRRC8A), a ubiquitously expressed but poorly characterized transmembrane protein with many leucine-rich repeats, as an essential component of the VRAC channel. We show that SWELL1 is localized to the plasma membrane and that its knockdown dramatically suppresses native VRAC currents in multiple cell types. This deficit can be rescued by expression of RNAi-insensitive SWELL1 complementary DNA (cDNA) clones. Mutagenesis analysis further suggests that SWELL1 is near or part of the pore of the VRAC channel complex.

RESULTS

Genome-wide RNAi Screen Identifies LRRC8A as Essential for Hypotonicity-Induced Iodide Influx

To search for genes encoding VRAC or its regulators, we developed a high-throughput cell-based fluorescence assay for $I_{Cl,\ swell}$ activity in 384-well format using an automated Fluorometric Imaging Plate Reader (FLIPR). HEK293T cells stably expressing the halide-sensitive yellow fluorescent protein (YFP) (Galietta et al., 2001) were first stimulated with hypotonic solutions for 5 min to elicit a large endogenous $I_{Cl,\ swell}$ current (Hélix et al., 2003). A subsequent addition of NaI triggered a rapid fluorescence decrease due to I^- influx through VRAC (Figure 1A). The degree of fluorescence quenching correlated with the strength of the hypotonic stimulus and reached a peak of ~70% reduction at a final osmolality of 215 mOsm/kg (Figure 1B; Table S1). The YFP quenching response was strongly inhibited by DCPIB (4-(2-butyl-6, 7-dichloro-2-cyclopentyl-indan-1-on-5-yl) oxobutyric acid), a potent VRAC antagonist (Decher et al., 2001), with an IC_{50} of 20.9 μM (Figure 1C). These data confirm the validity of this assay and indicate a large assay window. Cells transfected with small interfering RNA (siRNA) against several previously proposed VRAC candidates (ICln, CLC-2, CLC-3, and BEST1) (Hoffmann et al., 2009) showed normal hypotonicity-induced YFP quenching responses, similar to cells treated with scrambled siRNA (Figure S1 available online), indicating that these proteins are not by themselves required for VRAC activity in HEK293T cells.

To identify VRAC molecular components, we performed an unbiased genome-wide RNAi screen with an arrayed siRNA library (QIAGEN) targeting 17,631 known and 4,837 predicted human genes (Zhang et al., 2009) (see Experimental Procedures). We initially focused our attention on proteins predicted to have at least one transmembrane (TM) domain (a feature shared by all ion channels). The knockdown of ~500 such genes reduced hypotonicity-induced YFP quenching responses to various degrees. From this list, we manually inspected baseline fluorescence and hypotonicity-induced fluorescence changes to eliminate many false positives identified due to cell death or cell detachment upon knockdown. We picked 51 candidate genes with unknown or poorly defined function and evaluated them in a secondary RNAi screen using smartpool siRNAs (a mix of four individual siRNAs against different regions of the transcript) from a different source (Dharmacon). Knockdown of *LRRC8A* (*l*eucine-*r*ich *r*epeat-containing protein *8A*) caused a pronounced decrease of hypotonicity-induced YFP quenching (Figures 2A and 2B) without affecting the basal fluorescent levels of transfected cells (data not shown). The siRNA-mediated inhibition was as efficacious as the VRAC antagonist DCPIB. Attenuation of quenching responses was observed with individual siRNAs targeting distinct regions of the transcript (Figure 2C), suggesting an on-target mechanism of action of these siRNAs. All siRNAs tested reduced the abundance of the target transcripts as assayed with quantitative polymerase chain reaction (qPCR) (Figure S2A). Since *LRRC8A* (also called *LRRC8* or *AGM5*) appears to encode a protein required for an anion flux in response to cell swelling, we named this gene *SWELL1*.

SWELL1 Is Required for VRAC Channel Activity in Various Cell Types

We next used established conventional whole-cell patch-clamp recording protocols to assay $I_{Cl,\ swell}$ activity in the presence and absence of SWELL1 (Hélix et al., 2003; Lewis et al., 1993; Shen et al., 2000). Three days after transient transfection of HEK293T cells with scrambled siRNA or siRNA against *SWELL1*, cells from both conditions revealed similar low background conductance in isotonic solution indicating *SWELL1* siRNA treatment had no detectable influence on cell health (Figure 3A, Table S2). Hypotonic solutions elicited large increases in

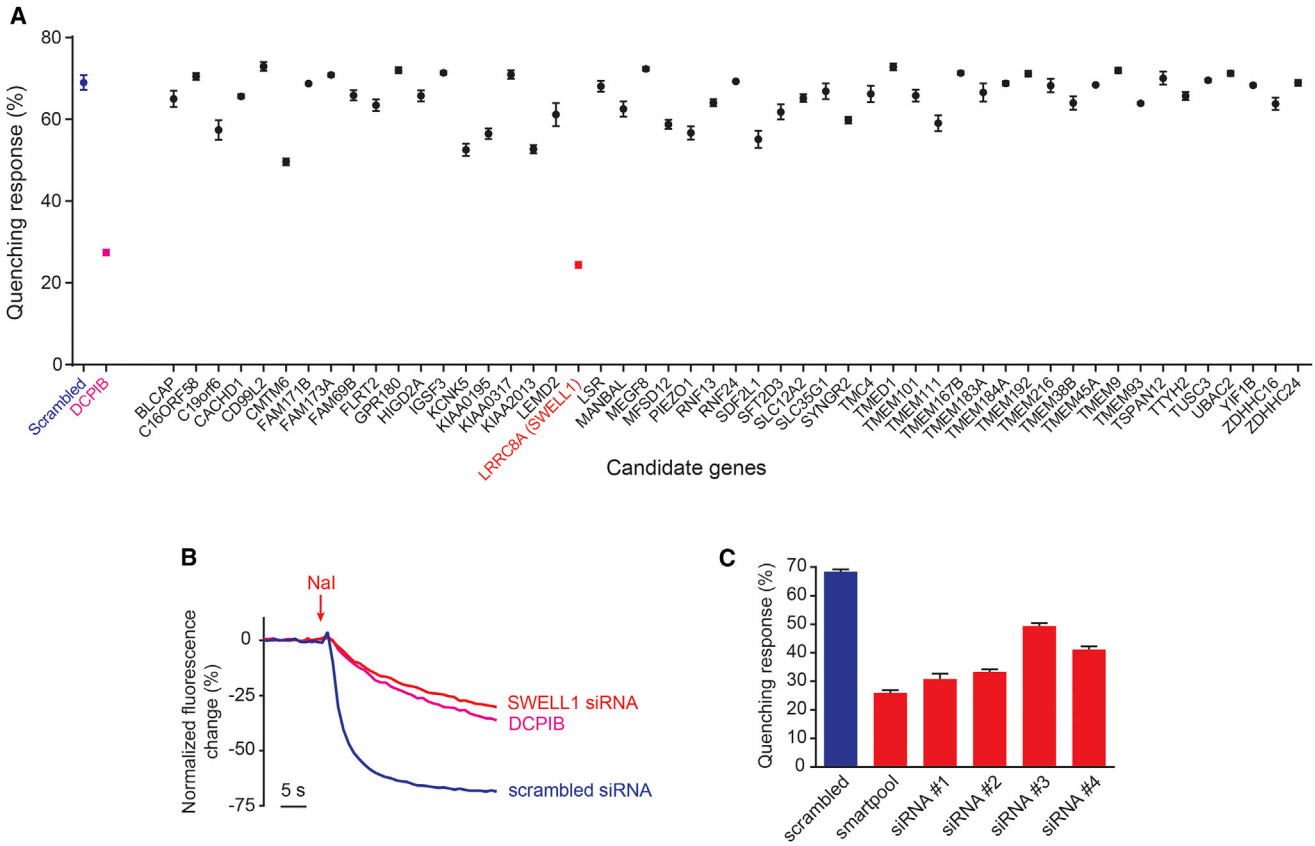

Figure 2. SWELL1 Is Essential for Hypotonicity-Induced Iodide Influx

(A) Hypotonicity-induced quenching responses (mean ± SEM, n = 3–4) in HEK-YFP cells transfected with scrambled siRNA or siRNA against 51 candidate genes.

(B) Representative traces of fluorescence change in HEK-YFP cells transfected with either scrambled siRNA or *SWELL1* siRNA. Cells treated with 50 μM DCPIB were used as a positive control.

(C) Hypotonicity-induced quenching responses (mean ± SEM; n = 4) in HEK-YFP cells transfected with either scrambled siRNA or various individual *SWELL1* siRNAs present in the smartpool.

See also Figure S2.

conductance in scrambled siRNA-transfected cells after a short lag (Figures 3A and 3B). These currents had characteristics typical of $I_{Cl,\ swell}$ (Figures S3A–S3E): voltage-independent block by DCPIB, voltage-dependent inhibition by DIDS (4,4' diisothiocyanatostilbene-2,2'-disulfonic acid), largely permeable to Cl^- (see Experimental Procedures) and mild outwardly rectifying. Remarkably, the response of *SWELL1* siRNA-treated cells to a hypotonic stimulus was dramatically suppressed (Figures 3A and 3B).

To test whether SWELL1 is also essential for VRAC channel activity in other cell types, we investigated $I_{Cl,\ swell}$ in both HeLa cells and primary human CD4+ T lymphocytes where VRAC was first recorded (Cahalan and Lewis, 1988). VRAC activity in both cell types had similar overall properties to those in HEK293T cells, including moderate outward rectification and block by DCPIB and DIDS (Figures S3F–S3L). Once again, we observed a robust suppression of VRAC by targeting *SWELL1* through siRNA transfection in HeLa cells (Figures 3C and 3D) and lentiviral transduction of short hairpin RNA (shRNA) in T lymphocytes (Figures 3E and 3F). Thus, endogenous $I_{Cl,\ swell}$ with typical VRAC features are dramatically inhibited by *SWELL1* knockdown in all three cell types tested.

Expression Profile and Localization of SWELL1

SWELL1 (LRRC8A) is predicted to contain 4 TM helices and 17 leucine-rich repeats and was first cloned from an agammaglobulinemia patient who lacked circulating B cells (Sawada et al., 2003). A heterozygous mutation, SWELL1$^{\Delta 91/+35}$ (91 C-terminal amino acids were replaced by 35 amino acids encoded by intron sequences), was proposed as the cause of the disease. SWELL1 is conserved across vertebrate species and four other homologous family members (LRRC8B-8E) are usually present in their genomes (Abascal and Zardoya, 2012; Kubota et al., 2004). The functions of SWELL1 and its family members are unknown. However, a recent sequence comparison analysis of their TM domains suggests that they are distantly related to pannexin ion channels (Abascal and Zardoya, 2012). RNAi knockdown of each of the four SWELL1 homologs had little effect on hypotonicity-induced YFP quenching responses (Figures S2B and S2C). This suggests that, unlike SWELL1, the other members

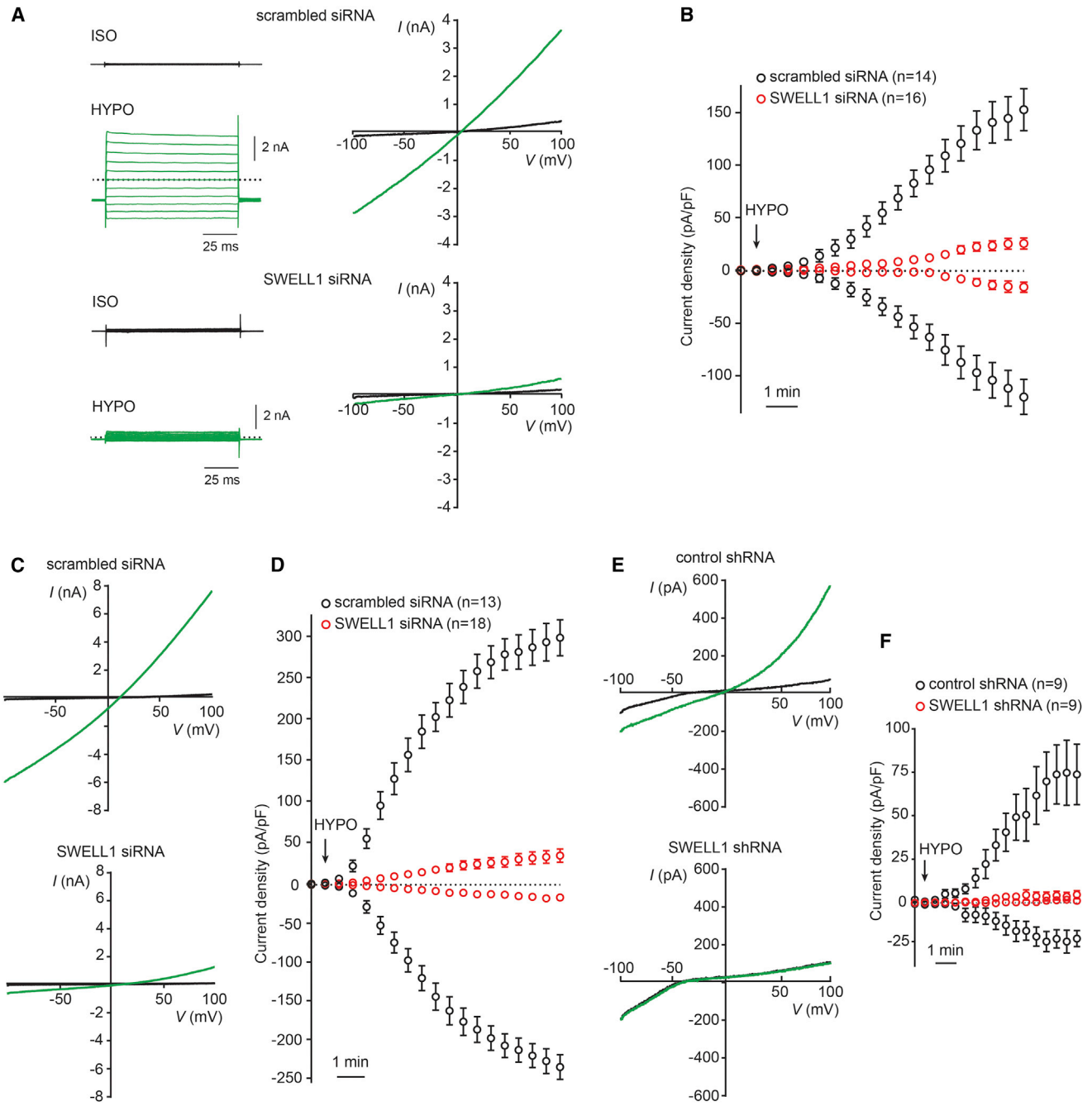

Figure 3. *SWELL1* Knockdown Abolishes Endogenous VRAC Currents in Multiple Cell Types

(A) Whole-cell currents monitored by voltage step (left) and ramp (right) protocols in isotonic solution (ISO; black traces) and after 6 min in hypotonic solution (210 mOsm/kg HYPO; green traces) shown for representative HEK293T cells transfected with either scrambled or *SWELL1* siRNA.

(B) Average current densities at −100 mV (below x axis) and +100 mV (above x axis) over time induced by the 210 mOsm/kg HYPO stimulus (applied at the arrow) for HEK293T cells.

(C) Whole-cell currents monitored by voltage ramp protocol from representative HeLa cells transfected with either scrambled or *SWELL1* siRNA in ISO (black trace) and 230 mOsm/kg HYPO (green trace) solutions.

(D) Average current densities at −100 mV and +100 mV over time induced by the 230 mOsm/kg HYPO stimulus (applied at the arrow) for HeLa cells.

(E) Whole-cell currents monitored by voltage ramp protocol from representative primary human CD4+ T lymphocytes transduced with lentiviruses expressing shRNAs targeting firefly luciferase (control) or *SWELL1* in ISO (black trace) and 260 mOsm/kg HYPO (green trace) solutions.

(F) Average current densities at −100 mV and +100 mV over time induced by the 260 mOsm/kg HYPO stimulus (applied at the arrow) for T lymphocytes.

Error bars represent mean ± SEM, and number of recorded cells is indicated for at least four separate experiments. Unapparent error bars are smaller than symbols. See also Figure S3 and Table S2.

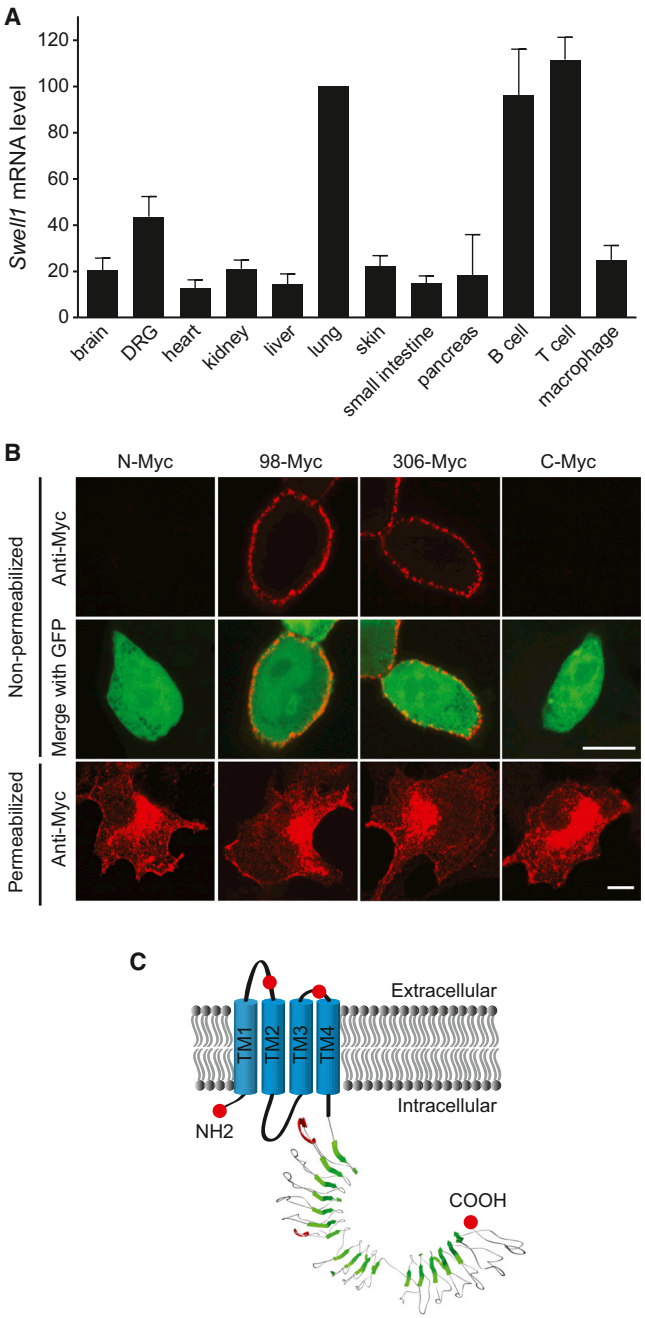

Figure 4. *Swell1* Is Expressed Broadly in Mouse Tissues and Is Present at the Plasma Membrane

(A) mRNA expression profile of murine *Swell1* determined by qPCR. *Gapdh* was used as the reference gene. Expression levels were normalized to lung as 100 and presented as mean ± SEM (n = 2–3). DRG: dorsal root ganglion.

(B) Nonpermeabilized and permeabilized HEK293T cells expressing SWELL1 with Myc tag inserted in various positions were immunostained with anti-Myc antibody. Scale bars: 5 μm.

(C) Schematic representation of the membrane topology of SWELL1 based on our results and the modeled structure of the LRR domains according to X-ray structure (Protein Data Bank ID 3cigA) of the homologous LRR domains of mouse Toll-like receptor 3. The sites of Myc tags (red circles) are indicated. See also Figure S4.

of this family are not by themselves essential for hypotonicity-induced iodide influx in HEK293T cells.

Swell1 mRNA was detected broadly in mouse tissues (Figure 4A) (Kubota et al., 2004), consistent with the ubiquitous presence of the VRAC channel. Relatively high expression of *Swell1* was observed in B and T cells, supporting a potential role in immune cell function (Sawada et al., 2003). If SWELL1 is a component of the VRAC channel complex, it should be present at the plasma membrane. To examine whether SWELL1 is expressed at the cell surface, we inserted Myc tags at several sites in the gene and transfected the constructs into HEK293T cells. The plasma membrane localization of SWELL1 was detected by immunofluorescent staining in intact (nonpermeabilized) cells expressing Myc-tagged constructs with the epitopes inserted after residues 98 (putative TM1-TM2 loop) or 306 (putative TM3-TM4 loop) (Figure 4B). In contrast, Myc tags located at either end of the protein were detected only after cell permeabilization (Figure 4B). These data suggest that contrary to previous suggestion (Sawada et al., 2003), the leucine-rich repeats of SWELL1 are in the cytoplasm (Figure 4C), confirming a recent bioinformatics prediction (Abascal and Zardoya, 2012).

SWELL1 Does Not by Itself Generate Larger VRAC Currents

Given that SWELL1 knockdown inhibited VRAC activation, we tested whether SWELL1 overexpression would enhance $I_{Cl,\ swell}$ current density. We transiently transfected HEK293T and HeLa cells with pIRES2-EGFP carrying the human *SWELL1* coding sequence (untagged) and recorded $I_{Cl,\ swell}$ from GFP-positive cells in the whole-cell configuration one day later. During hypotonic stimulation to either HEK293T (Figure S4A) or HeLa cells (data not shown) overexpressing SWELL1, $I_{Cl,\ swell}$ was not enhanced compared to that in control cells. On the contrary, SWELL1 overexpression resulted in decreased VRAC currents when assayed 2–3 days after transfection (data not shown). Expression of heterologous SWELL1 (FLAG-tagged) in HEK293T cells was verified by immunoprecipitation followed by western blot with an antibody against SWELL1 (Figure S4B). Note that this SWELL1 antibody was not sensitive enough to detect expression of endogenous SWELL1 in HEK293T or HeLa cells. These results indicate that extra SWELL1, although detected on the cell surface (Figure 4B), does not by itself generate larger $I_{Cl,\ swell}$. $I_{Cl,\ swell}$ amplitudes were not significantly diminished or enhanced upon overexpression of disease mutant SWELL1$^{\Delta 91/+35}$ (Figure S4A), suggesting that the mutant has no apparent dominant-negative or gain-of-function effect on VRAC activity in these cell lines.

SWELL1 Is a Component of the VRAC Channel Complex

To exclude the possibility of an off-target effect of *SWELL1* knockdown on VRAC activity, we performed cDNA rescue experiments in stable *SWELL1* knockdown cells. We transduced HeLa or HEK-YFP cells with lentiviruses carrying a *SWELL1* shRNA and established stable knockdown cell lines. We then transiently transfected RNAi-insensitive SWELL1 cDNA clones harboring five synonymous mutations within the shRNA target sequence and recorded whole-cell currents from transfected cells. As shown in Figure 5A, compared to vector

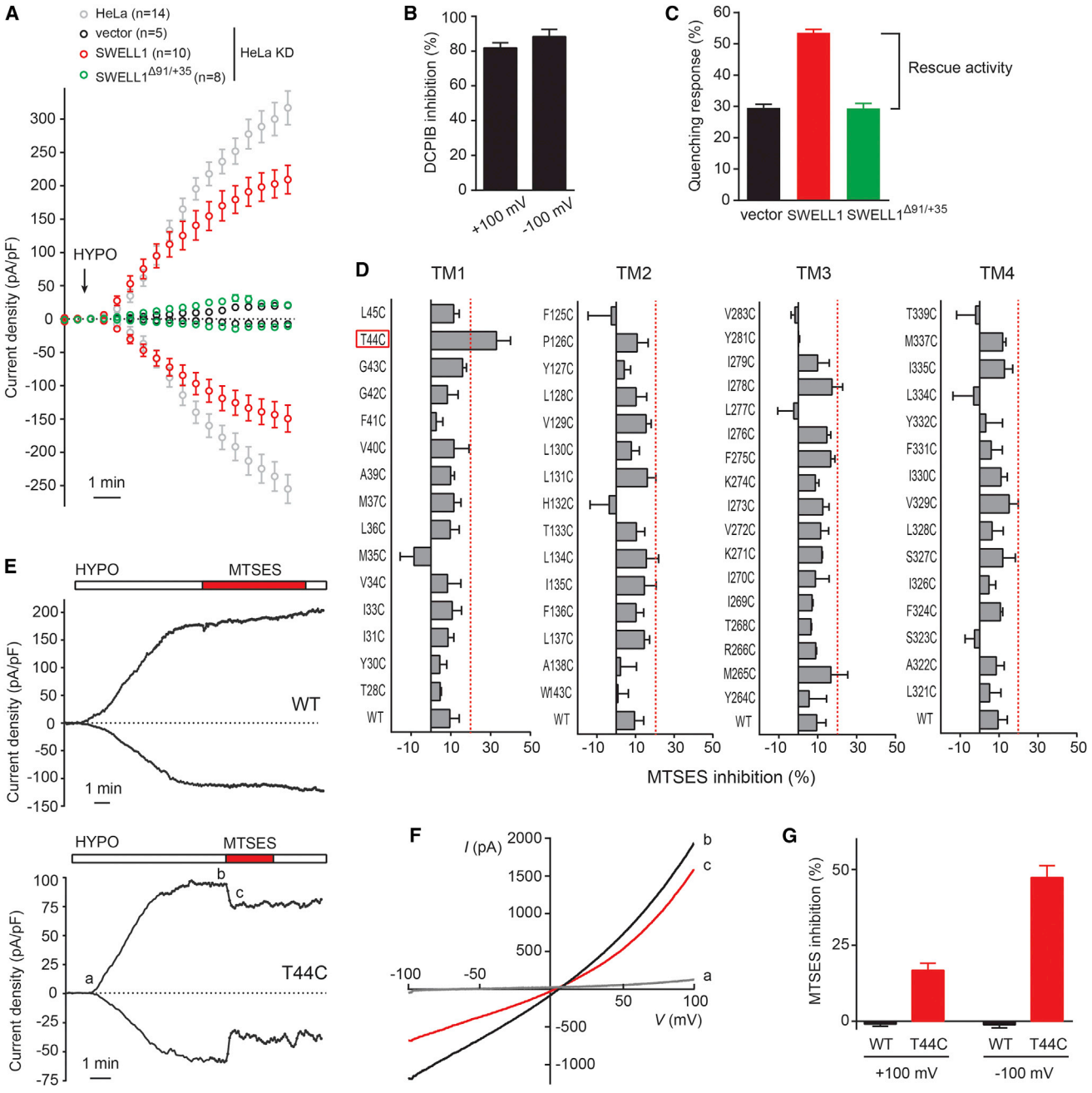

Figure 5. Currents Mediated by Cysteine Substitution of Threonine Residue (T44) in SWELL1 Are Acutely and Essentially Irreversibly Inhibited by the Application of Cysteine-Reactive MTSES

(A) Average current densities at −100 mV and +100 mV over time induced by the 230 mOsm/kg HYPO solution (applied at the arrow) for HeLa cells or stable *SWELL1* knockdown HeLa cells expressing RNAi-insensitive SWELL1 or SWELL1$^{\Delta 91/+35}$.

(B) HYPO-induced currents (n = 3) in stable *SWELL1* knockdown HeLa cells expressing RNAi-insensitive WT SWELL1 are strongly inhibited by DCPIB (20 μM).

(C) Hypotonicity-induced quenching responses (n = 4) in stable *SWELL1* knockdown HEK-YFP cells expressing RNAi-insensitive SWELL1 or SWELL1$^{\Delta 91/+35}$.

(D) Inhibition by MTSES application (n = 3–5) on the rescue activity of hypotonicity-induced quenching response in stable *SWELL1* knockdown HEK-YFP cells expressing RNAi-insensitive WT SWELL1 or SWELL1 mutants with cysteine individually substituted in four putative TM domains. Red dashed lines indicate two-fold background MTSES inhibition (18.9%) observed in WT SWELL1-mediated rescue activity. T44C (red box) is the only mutant whose rescue activity was significantly reduced by MTSES above the cut-off line.

(E) Representative examples of the effect of MTSES application (red) on hypotonicity-induced currents for stable *SWELL1* knockdown HeLa cells expressing RNAi-insensitive WT SWELL1 or SWELL1 (T44C).

(legend continued on next page)

alone, expression of RNAi-insensitive wild-type (WT) SWELL1 in stable knockdown HeLa cells restored hypotonicity-induced currents, which have many key features of parental $I_{Cl,\ swell}$, such as mild outward rectification and voltage independent inhibition by DCPIB (Figure 5B). Besides hypotonicity-induced cell swelling, VRAC is also activated by reduced intracellular ionic strength under constant-volume conditions (Voets et al., 1999). Consistent with SWELL1 being essential for VRAC activity, a reduction of intracellular ion strength activated DCPIB-sensitive currents in control cells, but not in *SWELL1* stable knockdown cells (Figures S5A–S5C and data not shown). Importantly, expression of RNAi-insensitive WT SWELL1 rescued this activity (Figures S5A–S5C). These data confirm that the observed RNAi phenotype is due to silencing of SWELL1.

Expression of RNAi-insensitive SWELL1$^{\Delta 91/+35}$ in stable knockdown cells failed to generate any $I_{Cl,\ swell}$ current above the background (Figure 5A), indicating that this mutation is not functional in this assay. We further performed a similar cDNA rescue experiment in stable *SWELL1* knockdown HEK-YFP cells using the fluorescence reporter assay. Consistent with the electrophysiological data, expression of WT SWELL1, but not disease mutant SWELL1$^{\Delta 91/+35}$, increased hypotonicity-induced iodide influx compared to vector control (Figure 5C). Our in vitro findings that SWELL1$^{\Delta 91/+35}$ mutant lacks VRAC function and exhibits no prominent dominant negative activity suggest that this ion channel might be involved in regulating the maturation of human B cells. Whether the heterozygous mutation that expresses the SWELL1$^{\Delta 91/+35}$ allele causes agammaglobulinemia by simple haploinsufficiency of SWELL1 or other possible mechanisms will have to be evaluated in the future (Sawada et al., 2003).

The evidence thus far suggests that SWELL1 is required for VRAC. SWELL1 could be part of VRAC channel complex; however, it is also possible that SWELL1 regulates VRAC activity indirectly, for example by controlling channel expression or trafficking. To distinguish these two possibilities, we used the substituted cysteine accessibility method (SCAM) to identify SWELL1 residues which when mutated to cysteine can react with a thiol-reactive reagent (Karlin and Akabas, 1998). If such reactions cause acute and irreversible alterations in the channel activity, it would suggest that SWELL1 is an integral component of the VRAC complex. For this purpose, we chose negatively charged membrane-impermeable 2-sulfonatoethyl methanethiosulfonate (MTSES) and observed no apparent effect of extracellular MTSES (3.33 mM) on $I_{Cl,\ swell}$ reconstituted by WT SWELL1 in stable knockdown HeLa cells (see below). This indicates that endogenous SWELL1 cysteines accessible from the extracellular side either do not react with MTSES or, if they do, do not interfere with channel activation.

We then systematically substituted cysteines individually into all four putative TM domains of SWELL1. To facilitate the SCAM screen, we took advantage of the fluorescence reporter assay in stable *SWELL1* knockdown HEK-YFP cells. We observed a small decrease (~10%) of WT SWELL1-mediated rescue activity by MTSES application during hypotonic stimulation (Figure 5D), which is likely a background response specific to this assay since no inhibition was detected by electrophysiological recordings (Figures 5E and 5G). Of the 76 mutants, 62 produced relatively normal cDNA rescue activities (defined as >60% of the activity mediated by WT SWELL1) (Figure S5D). We then screened the 62 functional mutants with MTSES application, and observed that cysteine replacement of threonine at position 44 (T44C) stood out, as MTSES substantially reduced its activity (Figure 5D). Whole-cell patch-clamp recordings of stable *SWELL1* knockdown HeLa cells expressing T44C revealed that extracellular MTSES rapidly suppressed T44C-mediated currents (Figure 5E, bottom). The effect persisted after MTSES washout (Figure S5E), consistent with covalent modification of the protein. MTSES-induced inhibition was more pronounced for inward currents (Cl^- efflux) than outward currents (Cl^- influx) (Figure 5E–5G), which made $I_{Cl,\ swell}$ more outwardly rectifying. These results, combined with the RNAi study, suggest that SWELL1 is an essential component of the VRAC complex.

Ion selectivity of a channel is determined by its pore, or in rare cases, by pore-associated subunits (Hille, 2001). Thus, the ability to change selectivity by a point mutation would provide strong evidence that SWELL1 forms or is at least very close to the VRAC channel pore. Since a permeability preference of $I^- > Cl^-$ is characteristic of VRAC, we estimated permeability ratios (P_I/P_{Cl}) from the difference in reversal potential (V_{rev}) observed where equimolar I^- or Cl^- was the only permeant extracellular anion. Endogenous $I_{Cl,\ swell}$ in HeLa cells and WT SWELL1-mediated rescue currents in stable knockdown cells were similar (P_I/P_{Cl}: ~1.3) (Figures 6A and 6C), confirming a preference for I^- over Cl^-. While V_{rev} in the Cl^--containing solution was similar (Figures 6A and 6B), V_{rev} in the I^- solution for T44C-mediated rescue currents was dramatically shifted to more negative potentials compared to WT SWELL1-mediated currents and endogenous $I_{Cl,\ swell}$ in HeLa cells (Figures 6A and 6B). These data indicate that T44C mutant is more permeable to I^- than controls (Figure 6C). The shift of V_{rev} in the I^- solution is not dependent on the current density (Figure S6). We also mutated T44 to an acidic (glutamic acid, E) or basic (arginine, R) residue to determine whether the anion permeability could be altered. Although T44E-mediated rescue currents were similar to controls (Figures 6A and 6C), currents from T44R showed a significant reduction of I^- selectivity (P_I/P_{Cl}: 1.15, Figures 6A–6C). Therefore, data from two independent substitutions argue that T44 has a sizeable impact on anion permeability. The mechanism of how the pore is affected by these mutations (e.g., side chain bulkiness or pKa) is beyond the scope of this current work but these data support the conclusion that SWELL1 is close to or forms the pore of the VRAC channel complex.

(F) Current traces acquired using a ramp protocol at the indicated time points in E (bottom) show outwardly rectifying hypotonicity-induced currents (b) are partially blocked after MTSES exposure (c).

(G) MTSES-induced block on recue currents mediated by WT SWELL1 (n = 13) and T44C (n = 10) at −100 mV and +100 mV.

Error bars represent mean ± SEM. See also Figure S5.

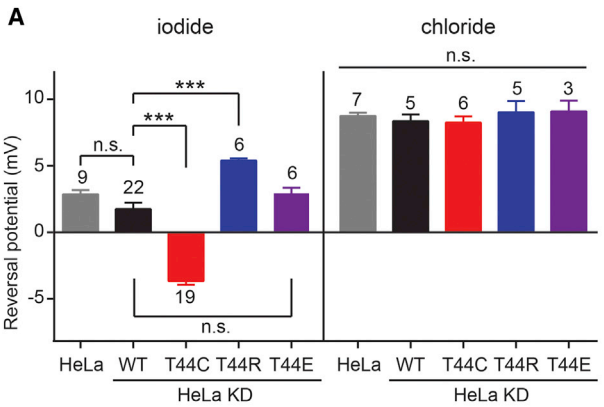

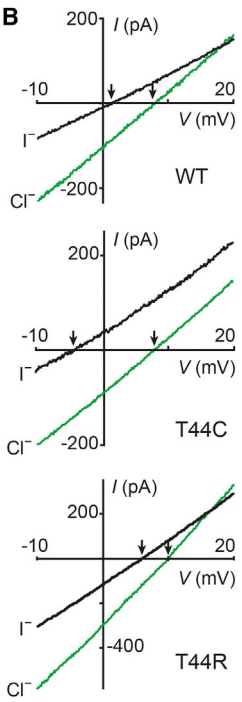

C

	HeLa	WT	T44C	T44R	T44E
P_I/P_{Cl}	1.26 (1.24, 1.28)	1.29 (1.26, 1.33)	1.59 (1.57, 1.63)	1.15 (1.12, 1.19)	1.27 (1.23, 1.32)

Figure 6. T44C and T44R Mutations of SWELL1 Alter the Anion Selectivity of $I_{Cl,\ swell}$

(A) Reversal potentials (V_{rev}) determined under identical conditions other than the extracellular anion (iodide or chloride) for VRAC currents recorded from HeLa cells or stable *SWELL1* knockdown HeLa cells expressing WT or mutated SWELL1. Bars represent mean ± SEM (***p < 0.001, n.s., not significant).

(B) *I-V* relationships recorded in extracellular I^- and Cl^- solutions in stable *SWELL1* knockdown HeLa cells expressing WT or mutated SWELL1. Arrows indicate V_{rev} for each cell. The larger the difference between V_{rev} in I^- and Cl^- solution, the larger the selectivity for I^- over Cl^-.

(C) P_I/P_{Cl} values were calculated based on the data shown in (A) (see Experimental Procedures). Values in parentheses indicate the compound SEM for the calculation.

See also Figure S6.

SWELL1 Contributes to Regulatory Volume Decrease

To test whether diminished $I_{Cl,\ swell}$ in *SWELL1* knockdown cells impair hypotonicity-induced RVD, we investigated HeLa cells which are widely used in cell volume regulation studies (Lang, 2007). No difference in cell volume with or without SWELL1 knockdown was observed prior to hypotonic stimulation (Figure S7A), suggesting that SWELL1 is not required for cell volume homeostasis under iso-osmotic conditions. The initial maximum volume increase after exposure to hypotonic solution was also the same in cells transfected with *SWELL1* siRNA compared to controls (Figure 7A, 1–3 min). However, cell volume recovery was significantly slower in cells treated with siRNA against *SWELL1* (Figures 7A and 7B). This highlights an essential function of SWELL1 in maintaining cell volume homeostasis upon hypotonic challenge. The remaining RVD activities are possibly due to residual SWELL1 protein expression and other ion efflux pathways, such as swelling-activated K^+ channels and K^+-Cl^- cotransporters (Hoffmann et al., 2009). Besides loss of intracellular electrolytes, hypotonicity-induced efflux of small organic osmolytes (such as taurine, an abundant amino acid derivative) also contributes to cell volume recovery. Although accumulating evidence suggests that these osmolytes might be released from cells through the VRAC channel, direct evidence is lacking due to its unknown molecular identity. We observed a sharp increase in the rate of taurine efflux after hypotonic stimulation in scrambled siRNA-treated HeLa cells, and *SWELL1* knockdown dramatically blunted this response (Figure 7C). We also tested if taurine permeates the VRAC channel (Manolopoulos et al., 1997). Hypotonicity-induced whole-cell outward currents were detected in HeLa cells but not in *SWELL1* stable knockdown cells when extracellular Cl^- was replaced by taurine (Figures S7B and S7C and data not shown). Expression of RNAi-insensitive WT SWELL1 rescued this activity (Figures S7B and S7C). These data are consistent with VRAC mediating hypotonicity-induced taurine flux in HeLa cells.

DISCUSSION

Through an unbiased genome-wide RNAi screen, we identify SWELL1, and show that this multipass transmembrane protein is an essential component of VRAC. The evidence to support this conclusion includes: (1) SWELL1 expression is required for the endogenous VRAC currents in various cell types, and for regulation of cell volume homeostasis; (2) SWELL1 is a plasma membrane protein, and its mRNA is broadly expressed in mammalian tissues and cells; and (3) point mutations in SWELL1 cause a significant change in a VRAC pore property, specifically I^- versus Cl^- selectivity.

The precise relation between SWELL1 and the VRAC channel pore remains unclear. We show that mutations at SWELL1 T44 affect VRAC anion selectivity. Although mutagenesis that causes a change in ion selectivity is often used as evidence that the site is within the pore, potential exceptions to this rule have been reported (Kaczmarek and Blumenthal, 1997). At least two possibilities exist. On the one hand, SWELL1 could be a VRAC subunit closely associated with the pore and required for modulating channel properties, including ion selectivity, similar to KCNE subunits (MinK family) of voltage-gated potassium channels (Kaczmarek and Blumenthal, 1997). On the other hand, SWELL1 could constitute a pore-forming subunit, which would be consistent with the prediction that LRRC8 proteins are evolutionarily related to pannexin channels. We confirmed experimentally that SWELL1 indeed contains four TM domains with cytoplasmic N and C termini, which is a basic structural feature shared by a superfamily of evolutionarily distinct and functionally diverse

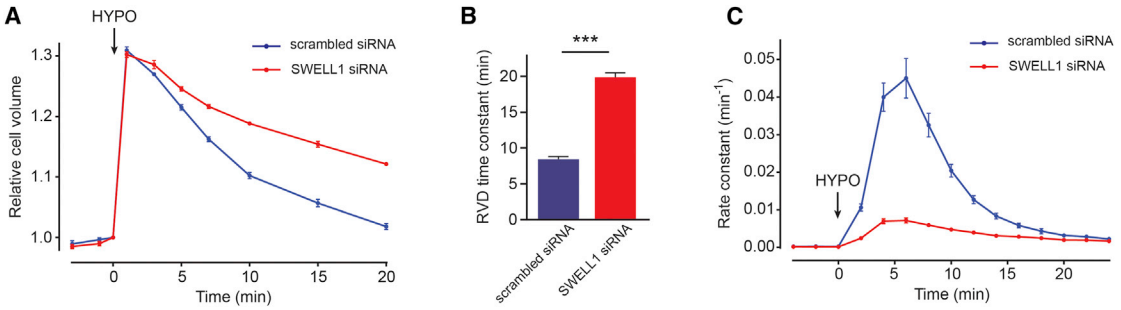

Figure 7. SWELL1 Contributes to Regulatory Volume Decrease and Is Required for Hypotonicity-Induced Taurine Release

(A) Time course of relative cell volume change after the exposure to hypotonic solution (220 mOsm/kg, indicated by the arrow) in HeLa cells transfected with either scrambled siRNA or siRNA against *SWELL1*. Each data point represents the mean ± SEM (n = 5).

(B) RVD time constants were determined using one-phase exponential decay curve fitting for data shown in (A). Bars represent mean ± SEM (***$p < 0.001$).

(C) Time course of the rate constant for swelling-induced [H^3]taurine efflux after the exposure of hypotonic solution (210 mOsm/kg, indicated by the arrow) in HeLa cells transfected with either scrambled siRNA or siRNA against *SWELL1*. Each data point represents the mean ± SEM (n = 3).

See also Figure S7.

ion channels, including pannexin (its invertebrate homolog innexin), gap junction-forming connexin, and more recently identified CALHM (calcium homeostasis modulator) families (Siebert et al., 2013). Interestingly, T44 of SWELL1 is predicted to be in the external portion of TM1, and the equivalent regions of connexins and pannexins are thought to line part of their pores based on X-ray crystal structure and SCAM analysis (Maeda et al., 2009; Wang and Dahl, 2010). Other than T44C, cysteine mutants in other regions of the four putative TM domains were not affected upon MTSES application. This could be explained by the low sensitivity of fluorescence assay we used, or the choice of MTSES as cysteine-reactive reagent. It is also possible that the remaining part of the VRAC pore is formed by other subunits (see below), or other regions of SWELL1 including the extracellular loops, or N or C terminus (as is the case for both connexins and pannexins) (Maeda et al., 2009; Wang and Dahl, 2010). Regardless, our data allow us to conclude that SWELL1 is an essential component of VRAC that is either pore-forming or is closely-associated with the pore.

Extra SWELL1 expression, although detected on the cell surface, did not induce larger $I_{Cl,\ swell}$. Overexpressing essential subunits of ion channels does not always lead to increased channel activity. There are various reasons for lack of sufficiency. For example, it could be due to a limiting factor upstream of VRAC channel activation, such as a putative cell volume sensor (it is not clear if VRAC itself senses cell volume change). Pore-forming ORAI1 ion channel is such an example, which requires the calcium sensor STIM1 to reconstitute store-operated calcium channel function (Cahalan, 2009). Alternatively, SWELL1 could be one of the subunits in a multimeric channel complex. In this scenario, the other subunit(s) could be the limiting factor(s) during overexpression, like in the case of pentameric hetero-oligomers of ligand-gated ion channels (Minier and Sigel, 2004). Future studies will determine the full molecular composition of the VRAC channel complex and the precise relation between SWELL1 and the channel pore.

In conclusion, the identification of SWELL1 as a long-sought VRAC component has allowed us to provide strong support for the contribution of the VRAC channel to cell volume regulation and hypotonicity-induced taurine efflux. Besides cell volume regulation, the VRAC channel is also implicated in many other processes including regulation of membrane potential, salt and fluid secretion, glutamate release, cell proliferation, and apoptosis (Nilius and Droogmans, 2003; Okada et al., 2009). This discovery will now enable further molecular characterization of this ion channel complex, as well as a genetic approach to understand its role in physiology and disease. In addition, our finding that an essential VRAC component belongs to the evolutionarily conserved LRRC8 family raises the question whether other LRRC8 family members are also associated with anion channels or transporters in vertebrate species.

EXPERIMENTAL PROCEDURES

Additional information regarding plasmids, siRNA library, cell culture, qPCR assay, and detailed procedures for western blot and electrophysiology are described in the Extended Experimental Procedures.

Hypotonicity-Induced YFP Quenching Assay

A cell-based assay using the halide-sensitive YFP (with H148Q and I152L mutations) was described previously (Galietta et al., 2001). HEK293T cells were transfected with the plasmid carrying the halide-sensitive YFP. Stably transfected and single-cell derived clones (HEK-YFP) were isolated by FACS. HEK-YFP cells in 384 well plates were washed and kept in 20 μl/well isotonic solution (in mM): 140 NaCl, 5 KCl, 20 HEPES (310 mOsm/kg; pH 7.4 with NaOH). A serial dilution of hypotonic solutions was made by omitting NaCl and adding different amounts of mannitol (Table S1). Osmolalites of all the solutions were measured by Vapor Pressure Osmometer 5600. We stimulated cells with 20 μl/well hypotonic solutions for 5 min, followed by addition of 10 μl/well 200 mM NaI. FLIPR (Molecular Devices) recorded fluorescence in each well simultaneously during the assay. The fluorescence reading at 20 s after NaI addition was normalized to that at 5 s before the addition (set as 100%). The percentage of fluorescence decrease after NaI addition was calculated as the YFP quenching response. All subsequent YFP quenching assays (except the initial experiment in Figure 1A) used hypotonic solution (in mM): 5 KCl, 20 HEPES, 90 mannitol (120 mOsm/kg). For the SCAM screen, we incubated SWELL1 cDNA-rescued cells with 10 mM MTSES in hypotonic solution for 5 min before the regular FLIPR assay described above. For siRNA transfection in 384-well plates, we first added 20 μl Opti-MEM with 0.15 μl Lipofectamine RNAiMAX (Life Technologies) and 1 pmol smartpool siRNAs (Dharmacon) to each well, incubated them for 20 min, and added 20 μl of HEK-YFP

cells (10^4 cells/well). The cells were incubated at 37°C for 3 days before the assay.

Genome-wide RNAi Screen

The siRNA library (QIAGEN) was previously described (Zhang et al., 2009). siRNA transfections for a total of 292 plates in HEK-YFP cells were performed as described above except using a GNF robotic system. The hypotonicity-induced YFP quenching response was calculated and then normalized to the plate average (set as 1). The average score of two duplicates was determined for each well. The well was considered a hit when its score was 2 standard deviations below the mean. For the follow-up RNAi screen, we transfected cells with smartpool siRNAs (Dharmacon) against 51 candidate genes encoding putative membrane proteins, and assayed for the hypotonicity-induced YFP quenching response. As controls, scrambled siRNA duplexes (QIAGEN) were employed.

Cell Culture

Cells were maintained in standard culture conditions. For siRNA experiments, cells were cotransfected with 25 nM siRNA and 500 ng/ml GFP vector using Lipofectamine 2000 (Life Technologies) to identify transfected cells, seeded on 12 mm diameter poly-D-lysine coated glass coverslips (BD) in 24-well dishes, and were recorded 3 days after transfection. For SWELL1 overexpression experiments, 500 ng/ml SWELL1 or SWELL1$^{\Delta 91/+35}$ pIRES2-EGFP constructs or pIRES2-EGFP vector were transfected and cells were recorded 18–30 hr later.

Lentivrial shRNA and Stable Knockdown

SWELL1 shRNA with the same sequence as the most potent siRNA (#1) was inserted into pLL3.7 and pLKO.1 vector (Addgene). Lentiviruses were produced by cotransfecting HEK293T cells with SWELL1 shRNA constructs, pMD2.G, pRSV-REV, and pMDL.RRE following Addgene's instruction. Primary CD4+ lymphocytes were transduced with SWELL1 shRNA lentiviruses (pLL3.7 based) using RetroNectin reagent as described by the manufacturer (Takara), and infected cells (GFP+) were recorded 3 days after transduction. We used lentiviruses carrying shRNA targeting luciferase gene as controls. HeLa or HEK-YFP cells were transduced with SWELL1 shRNA lentiviruses (pLKO.1 based), selected with puromycin (2 μg/ml) 48 hr posttransduction for 2 weeks. Stable knockdown cell lines were derived from single-cell colonies and used for cDNA rescue experiments. Knockdown was assessed by qPCR.

Electrophysiology

Whole-cell patch-clamp recordings were performed as described (Dubin et al., 2012), except that standard methods to achieve low access resistance (R_a) were performed and solutions were adapted from previous studies (Hélix et al., 2003; Jackson and Strange, 1996; Shen et al., 2000). Cells were continuously perfused with extracellular solution (in mM): 90 NaCl, 2 KCl, 1 $MgCl_2$, 1 $CaCl_2$, 10 HEPES, 110 mannitol (300 mOsm/kg; pH 7.4 with NaOH). Hypotonic solutions (HYPO) had the same ionic composition but contained either 10 mM (HEK293T) or 30 mM (HeLa) or 60 mM (lymphocytes) mannitol instead of 110 mM. When HYPO was applied, only one cell was tested per coverslip. Recording pipettes were usually filled with intracellular solution containing (in mM) 133 CsCl, 5 EGTA, 2 $CaCl_2$, 1 $MgCl_2$, 10 HEPES, 4 Mg-ATP, 0.5 Na-GTP (pH 7.3 with CsOH; 106 nM free Ca^{2+}) and had resistances of 2–3 MΩ. For lymphocyte recordings and initial Cl^- dependence studies, the intracellular solution contained (in mM): 40 CsCl, 100 gluconate, 1 $MgCl_2$, 1.93 $CaCl_2$, 5 EGTA, 10 HEPES, 4 Na_2-ATP, 0.5 Na-GTP (pH 7.3 with CsOH). The reversal potential of $I_{Cl,\ swell}$ was +10.0 ± 1.3 mV (n = 21) where E_{Cl} = +9.5 mV (139 mM intracellular Cl^-), and −18.2 ± 4.2 mV (n = 3) in gluconate-containing intracellular solution where E_{Cl} = −16 mV (50.6 mM intracellular Cl^-), indicating a large contribution of Cl^- to the currents.

For bianionic experiments, recording pipettes contained 140 CsCl/10 HEPES/4 Mg-ATP (required for VRAC activity), pH 7.3 and 88 Na-X/10 HEPES/mannitol (110 or 30 mM), pH 7.4 was bath applied, where X was either Cl^- or I^-. An agar bridge containing 1 M KCl connected the headstage ground to the bath. Families of currents were elicited by 100 or 840 ms steps from a −50 mV (50 ms) prepulse potential to +120 to −120 mV in −20 mV increments every 10 s to determine voltage-dependent activation and inactivation properties of currents before and after challenge with HYPO. The holding potential was 0 mV. VRAC currents in HYPO were slowly inactivating at positive potentials. Voltage ramps were applied every 5 s from −100 to +100 mV at a ramp speed 1.1 mV/ms. Sampling interval: 50 μs; filter: 10 KHz.

For the SCAM analysis, solutions containing MTSES (0.1–3.33 mM) were bath applied near the plateau of $I_{Cl,\ swell}$ for 2–5 min. MTSES decreased T44C-mediated rescue currents with a latency of ~20 s. The percent block between 30–90 s was determined either by fitting the activation curves and comparing the fit current magnitude to the actual data (when MTSES was applied prior to current plateau) or by using current values just prior to MTS exposure (when MTSES arrived during a plateau). MTSES was washed out and the current recovery was determined by using either the fitted curve data points or the plateau current data. Data were analyzed offline using PClamp Clampfit10 and GraphPad Prism 6. P_I/P_{Cl} was determined using the equation = exp (($-(V_{rev,\ I-} - V_{rev,\ Cl-})$)*1/25.693) (Shen et al., 2000). The compound error in this difference calculation was determined as described in (Taylor, 1982).

Quantitative Real-Time PCR

Total RNA was reverse transcribed to generate cDNA, which was then used as templates for real-time PCR on ABI 7900HT fast real time system. Gene expression was normalized to *GAPDH*.

Immunostaining

Immunostaining was performed as previously described (Schmidt et al., 2009). For live-cell staining, cells were incubated with anti-Myc (9E11) antibody (1:50; Santa Cruz Biotech) at 37°C for 20 min followed by incubation with secondary antibody at room temperature for 10 min. Cells were then fixed with 2% paraformaldehyde (PFA). For regular immunocytochemistry, cells were fixed with 4% PFA, incubated with anti-Myc antibody (1:500) for 2 hr and secondary antibody for 1 hr. Coverslips were mounted and imaged with Nikon C2 confocal microscope.

Western Blot Analysis

Immunoprecipitation and western blot were performed by standard protocols with antibodies (Sigma) against FLAG tag (F3165) and SWELL1 (HPA016811).

Regulatory Volume Decrease

HeLa cells were transfected with 25 nM scrambled siRNA or siRNA against *SWELL1* in 24-well plate using Lipofectamine RNAiMAX. Three days post-transfection, siRNA-transfected cells were digested and suspended in 11.5 ml PBS. Cell volume was measured by the Z2 Coulter counter (Beckman Coulter). Cells within the diameter range of 10–25 μm (corresponding to a cell volume range of 524–8,181 fL) were counted and the average cell volume of more than 10,000 cells in each counting run was recorded. After three measurements, 8 ml hypotonic solution (the same as used in the RNAi screen) was added to the cell suspension and a series of measurements was taken until the restoration of the initial volume for cells treated with scrambled siRNA. The average cell volume one min before the hypotonic stimulus was normalized as 1 and the relative average volume at other time points was calculated. RVD time constants were determined using one-phase exponential decay curve fitting (GraphPad Prism 6).

Taurine Efflux Assay

Taurine efflux assay was performed as described previously (Falktoft and Lambert, 2004). siRNA-transfected HeLa cells in six-well plates were loaded with culture medium containing [^{3}H]taurine (2 μCi/ml) at 37°C for 2 hr. The cells were washed five times with isotonic solution (in mM): 145 NaCl, 2 KCl, 1 $MgCl_2$, 1 $CaCl_2$, 10 HEPES, pH 7.4 (adjusted with NaOH). Hypotonic solution was made by decreasing NaCl concentration to 95 mM. The experiment was performed by removal/addition of 1 ml aliquots of solutions at 2 min intervals. The efflux was initiated by aspiration of isotonic solution followed by addition of hypotonic solution. The cells were lysed at the end of the experiment with 0.5 M NaOH. The total ^{3}H activity in the cells was estimated as the sum of ^{3}H activity in all efflux samples and the final lysates using a Beckman Coulter LS 6500 liquid scintillation counter. The natural logarithm to the fraction of ^{3}H

activity remaining in the cells was plotted versus time, and the rate constant for the taurine efflux (min^{-1}) at each time point was subsequently estimated as the negative slope of the curve between the time point and the proceeding time point (Falktoft and Lambert, 2004).

Data Analysis

Statistical significance was evaluated using unpaired two-tailed Student's t test for comparing difference between two samples.

SUPPLEMENTAL INFORMATION

Supplemental Information includes Extended Experimental Procedures, seven figures, and two tables and can be found with this article online at http://dx.doi.org/10.1016/j.cell.2014.03.024.

ACKNOWLEDGMENTS

We thank Paul Groot-Kormelink for information on the HEK-YFP cell line; Yingyao Zhou and Jeff Janes for help with RNAi screen data analysis; Michael Bandell, Jie Xu, Swetha Murthy, Matt Petrus, Albert Parker, Angelica Romero, and Myleen Medina for technical assistance; Qiangfeng Zhang for 3D structural modeling; and members of the Patapoutian lab for valuable discussions. This work was supported by a grant from the NIH (R01 DE022115 to A.P.). A.P. is a Howard Hughes Medical Institute investigator.

Received: January 10, 2014
Revised: February 24, 2014
Accepted: March 18, 2014
Published: April 10, 2014

REFERENCES

Abascal, F., and Zardoya, R. (2012). LRRC8 proteins share a common ancestor with pannexins, and may form hexameric channels involved in cell-cell communication. Bioessays *34*, 551–560.

Ackerman, M.J., Wickman, K.D., and Clapham, D.E. (1994). Hypotonicity activates a native chloride current in Xenopus oocytes. J. Gen. Physiol. *103*, 153–179.

Cahalan, M.D. (2009). STIMulating store-operated Ca(2+) entry. Nat. Cell Biol. *11*, 669–677.

Cahalan, M.D., and Lewis, R.S. (1988). Role of potassium and chloride channels in volume regulation by T lymphocytes. Soc. Gen. Physiol. Ser. *43*, 281–301.

Chien, L.T., and Hartzell, H.C. (2007). Drosophila bestrophin-1 chloride current is dually regulated by calcium and cell volume. J. Gen. Physiol. *130*, 513–524.

Chien, L.T., and Hartzell, H.C. (2008). Rescue of volume-regulated anion current by bestrophin mutants with altered charge selectivity. J. Gen. Physiol. *132*, 537–546.

Decher, N., Lang, H.J., Nilius, B., Brüggemann, A., Busch, A.E., and Steinmeyer, K. (2001). DCPIB is a novel selective blocker of I(Cl,swell) and prevents swelling-induced shortening of guinea-pig atrial action potential duration. Br. J. Pharmacol. *134*, 1467–1479.

Doroshenko, P., and Neher, E. (1992). Volume-sensitive chloride conductance in bovine chromaffin cell membrane. J. Physiol. *449*, 197–218.

Dubin, A.E., Schmidt, M., Mathur, J., Petrus, M.J., Xiao, B., Coste, B., and Patapoutian, A. (2012). Inflammatory signals enhance piezo2-mediated mechanosensitive currents. Cell Rep *2*, 511–517.

Falktoft, B., and Lambert, I.H. (2004). Ca2+-mediated potentiation of the swelling-induced taurine efflux from HeLa cells: on the role of calmodulin and novel protein kinase C isoforms. J. Membr. Biol. *201*, 59–75.

Galietta, L.J., Haggie, P.M., and Verkman, A.S. (2001). Green fluorescent protein-based halide indicators with improved chloride and iodide affinities. FEBS Lett. *499*, 220–224.

Grinstein, S., Clarke, C.A., Dupre, A., and Rothstein, A. (1982). Volume-induced increase of anion permeability in human lymphocytes. J. Gen. Physiol. *80*, 801–823.

Hélix, N., Strøbaek, D., Dahl, B.H., and Christophersen, P. (2003). Inhibition of the endogenous volume-regulated anion channel (VRAC) in HEK293 cells by acidic di-aryl-ureas. J. Membr. Biol. *196*, 83–94.

Hille, B. (2001). Ion Channels of Excitable Membranes (Sunderland, MA: Sinauer Associates).

Hoffmann, E.K., Lambert, I.H., and Pedersen, S.F. (2009). Physiology of cell volume regulation in vertebrates. Physiol. Rev. *89*, 193–277.

Jackson, P.S., and Strange, K. (1996). Single channel properties of a volume sensitive anion channel: lessons from noise analysis. Kidney Int. *49*, 1695–1699.

Jentsch, T.J., Stein, V., Weinreich, F., and Zdebik, A.A. (2002). Molecular structure and physiological function of chloride channels. Physiol. Rev. *82*, 503–568.

Kaczmarek, L.K., and Blumenthal, E.M. (1997). Properties and regulation of the minK potassium channel protein. Physiol. Rev. *77*, 627–641.

Karlin, A., and Akabas, M.H. (1998). Substituted-cysteine accessibility method. Methods Enzymol. *293*, 123–145.

Kubota, K., Kim, J.Y., Sawada, A., Tokimasa, S., Fujisaki, H., Matsuda-Hashii, Y., Ozono, K., and Hara, J. (2004). LRRC8 involved in B cell development belongs to a novel family of leucine-rich repeat proteins. FEBS Lett. *564*, 147–152.

Lang, F. (2007). Mechanisms and significance of cell volume regulation. J. Am. Coll. Nutr. *26* (Suppl), 613S–623S.

Lewis, R.S., Ross, P.E., and Cahalan, M.D. (1993). Chloride channels activated by osmotic stress in T lymphocytes. J. Gen. Physiol. *101*, 801–826.

Maeda, S., Nakagawa, S., Suga, M., Yamashita, E., Oshima, A., Fujiyoshi, Y., and Tsukihara, T. (2009). Structure of the connexin 26 gap junction channel at 3.5 A resolution. Nature *458*, 597–602.

Manolopoulos, V.G., Voets, T., Declercq, P.E., Droogmans, G., and Nilius, B. (1997). Swelling-activated efflux of taurine and other organic osmolytes in endothelial cells. Am. J. Physiol. *273*, C214–C222.

Minier, F., and Sigel, E. (2004). Techniques: Use of concatenated subunits for the study of ligand-gated ion channels. Trends Pharmacol. Sci. *25*, 499–503.

Nilius, B., and Droogmans, G. (2003). Amazing chloride channels: an overview. Acta Physiol. Scand. *177*, 119–147.

Nilius, B., Oike, M., Zahradnik, I., and Droogmans, G. (1994). Activation of a Cl- current by hypotonic volume increase in human endothelial cells. J. Gen. Physiol. *103*, 787–805.

Okada, Y. (1997). Volume expansion-sensing outward-rectifier Cl- channel: fresh start to the molecular identity and volume sensor. Am. J. Physiol. *273*, C755–C789.

Okada, Y., Oiki, S., Hazama, A., and Morishima, S. (1998). Criteria for the molecular identification of the volume-sensitive outwardly rectifying Cl- channel. J. Gen. Physiol. *112*, 365–367.

Okada, Y., Sato, K., and Numata, T. (2009). Pathophysiology and puzzles of the volume-sensitive outwardly rectifying anion channel. J. Physiol. *587*, 2141–2149.

Sawada, A., Takihara, Y., Kim, J.Y., Matsuda-Hashii, Y., Tokimasa, S., Fujisaki, H., Kubota, K., Endo, H., Onodera, T., Ohta, H., et al. (2003). A congenital mutation of the novel gene LRRC8 causes agammaglobulinemia in humans. J. Clin. Invest. *112*, 1707–1713.

Schmidt, M., Dubin, A.E., Petrus, M.J., Earley, T.J., and Patapoutian, A. (2009). Nociceptive signals induce trafficking of TRPA1 to the plasma membrane. Neuron *64*, 498–509.

Shen, M.R., Droogmans, G., Eggermont, J., Voets, T., Ellory, J.C., and Nilius, B. (2000). Differential expression of volume-regulated anion channels during cell cycle progression of human cervical cancer cells. J. Physiol. *529*, 385–394.

Siebert, A.P., Ma, Z., Grevet, J.D., Demuro, A., Parker, I., and Foskett, J.K. (2013). Structural and functional similarities of calcium homeostasis modulator 1 (CALHM1) ion channel with connexins, pannexins, and innexins. J. Biol. Chem. *288*, 6140–6153.

Stotz, S.C., and Clapham, D.E. (2012). Anion-sensitive fluorophore identifies the Drosophila swell-activated chloride channel in a genome-wide RNA interference screen. PLoS ONE *7*, e46865.

Strange, K., Emma, F., and Jackson, P.S. (1996). Cellular and molecular physiology of volume-sensitive anion channels. Am. J. Physiol. *270*, C711–C730.

Taylor, J.R. (1982). An Introduction to Error Analysis: The Study of Uncertainties in Physical Measurements (Sausalito, CA: University Science Books).

Voets, T., Droogmans, G., Raskin, G., Eggermont, J., and Nilius, B. (1999). Reduced intracellular ionic strength as the initial trigger for activation of endothelial volume-regulated anion channels. Proc. Natl. Acad. Sci. USA *96*, 5298–5303.

Wang, J., and Dahl, G. (2010). SCAM analysis of Panx1 suggests a peculiar pore structure. J. Gen. Physiol. *136*, 515–527.

Zhang, E.E., Liu, A.C., Hirota, T., Miraglia, L.J., Welch, G., Pongsawakul, P.Y., Liu, X., Atwood, A., Huss, J.W., 3rd, Janes, J., et al. (2009). A genome-wide RNAi screen for modifiers of the circadian clock in human cells. Cell *139*, 199–210.